

---

# 3-6 Quantum Network Consisting of Laser-cooled Ions and Photons

**HAYASAKA Kazuhiro, KELLER Matthias, LANGE Birgit, LANGE Wolfgang, and WALTHER Herbert**

Peculiar states, such as superposition, quantum entanglement, have no counterparts in classical mechanics, and are of characteristic of quantum mechanics. Quantum networks are those in which the quantum states are faithfully communicated. Applications of quantum networks include distributed quantum computation connecting small-sized quantum computers, quantum bit commitment based on quantum entanglement, and quantum authentication that enables votes and transactions with assured security on personal information. We report studies at NICT towards a working prototype of quantum network consisting of laser-cooled ions and photons.

## **Keywords**

Quantum network, Quantum state, Superposition, Quantum interface, Quantum entanglement, Quantum teleportation

## **1 Introduction**

Quantum mechanics deals with peculiar states, such as superposition and quantum entanglement, which have no counterparts in classical mechanics. Quantum networks are those in which these quantum states are faithfully communicated. Applications of quantum networks include distributed quantum computation connecting quantum computers, quantum bit commitment based on quantum entanglement, and quantum authentication, which enables applications such as voting and financial transactions with assured security for personal information. These highly anticipated applications to information and communication protocols are possible only using quantum states, which do not exist in classical mechanics[1]. However, realizing quantum networks requires communication devices that can implement quantum mechanics in a manner that will faithfully transmit and convert the quantum states.

Various combinations of carriers have

been proposed for the physical system that will constitute quantum networks — for example, light[2], atoms and photons[3], and electron spins in solids and photons[4]. A quantum network can be constructed with light alone. However, it has also been suggested that a configuration combining photons and quantum materials will enable complicated quantum communication protocols, with the photons transmitting the quantum states as “flying qubits” and the quantum materials assigned to quantum memory and quantum operations as “stationary qubits”[3]. Atomic gases are not as practical as spins in solids in terms of fabrication of the necessary devices. However, they are easy to handle in the laboratory and are considered to form a suitable physical system for the implementation and verification of a prototype quantum network.

Generally, the term “atom” refers to a neutral atom or an atomic ion. There are established methods for controlling the motion of each atomic ion by electric field control and laser cooling. Various small-scale quantum

---

computations have been implemented using individual ions as qubits[5]. Recently, single photons were successfully generated from a single ion using a method based on Cavity Quantum Electrodynamics (Cavity QED)[6]. This is considered to be the physical system closest to implementation of an atom/photon quantum network. Here, we report in particular on experiments related to laser-cooled ions.

## 2 Laser-cooled ion-photon and quantum network

A quantum network based on laser-cooled ions and photons consists of quantum computers made of two or more ions. These quantum computers are placed as quantum nodes, and the photons connect the nodes as quantum channels.

It is relatively easy to trap an ion at a point in space without perturbation. It is also characteristic of ions that their interactions can be controlled easily using center-of-mass oscillation in an ion trap. These characteristics render the ion suitable for use in a physical system for quantum state memory and quantum computation[3]. Quantum state memory requires long coherence time. For example, a coherence time over 10 minutes has been observed for a  $^{171}\text{Yb}^+$  cloud with Ramsey spectroscopy[7]. This value suggests the possibility that laser-cooled ions may function as quantum memory. As a qubit, a coherence time over 10 seconds has been observed for  $^9\text{Be}^+$  ions[8]. In terms of quantum computation various small-scale quantum computations have been implemented based on a so-called Cirac-Zoller ion-trap quantum computer[9]. These implementations demonstrate that ions can form physical systems suitable for quantum computation. Major examples include control NOT gates, quantum teleportation of ionic quantum states, quantum error correction, semi-classical quantum Fourier transform, spectroscopy based on quantum logic, Grover's search algorithm, and generation of eight-ion quantum entanglement[5].

Quantum memory and small-scale quan-

tum computation based on laser-cooled ions are implemented in a limited region within several tens of micrometers in a single ion trap device. If we try to construct a quantum network using only ions, vacuum chambers containing ion traps will need to extend in all directions, in which the ions carrying the quantum states will then move. This is neither easy nor practical. On the other hand, photons have weak interactions with other physical systems and they propagate at the speed of light, and as a result are regarded as suitable for the transmission of quantum states[3]. Thus we do not try to move the ions themselves but instead connect the ions with photons that carry the quantum states of the ions. In this manner, we believe that it is possible to construct a quantum network that takes advantage of the characteristics of both ions and photons.

Now that small-scale quantum computations have succeeded, the recent topic of ion-trap quantum computation arises in the context of implementation of larger-scale computation[5]. We believe that the laser-cooled ion-photon quantum network will prove an important means of connecting small quantum computers in the implementation of large-scale computation. If we view quantum communication by photons as the main part of the system, we can further conclude that the laser-cooled ion-photon quantum network will also be an important means of using ions as a quantum computer for error-correction, as well as quantum memory for synchronization.

### 2.1 Atom-photon quantum interface based on cavity QED

A quantum network based on atoms and photons transfers the quantum states of atoms in the transmitting node to the quantum states of photons. The network then transmits the photons and transfers back the quantum states of the photons to the quantum states of the atoms in the receiving node. In this manner, a quantum network is constructed. The most basic quantum state is the superposition of two-level energy states—in other words, a

qubit. Denoting the eigenstate of the atom as  $(|0\rangle_{at}, |1\rangle_{at})$  and the eigenstate of the photon as  $(|0\rangle_{ph}, |1\rangle_{ph})$ , the bit transfer from an atom to a photon is expressed as in the following equation.

$$(\alpha|0\rangle_{at} + \beta|1\rangle_{at}) \otimes |0\rangle_{ph} \rightarrow |0\rangle_{at} \otimes (\alpha|0\rangle_{ph} + \beta|1\rangle_{ph}) \quad (1)$$

To transfer the quantum state means to transfer the coefficients of superposition from one physical system to another physical system. Note that the superposition does not remain in the atomic system after the transfer. The connection between different physical systems in quantum states is referred to as the quantum interface.

The most promising candidate quantum interface for mutual conversion of the superposition of the atom and the superposition of the photon is a method based on cavity QED, which was proposed by Cirac, Zoller, Kimble, Mabuchi [10]. As shown in Fig. 1, this method couples a three-level atom and an optical microcavity (referred to simply as the “cavity” hereafter) with the coupling constant  $g$  and irradiates an appropriately shaped laser pulse,  $\Omega(t)$ . This generates a single photon out of the cavity. The generated photon maintains the superposition of the atom and produces the quantum interface, as indicated by Equation (1). A time-reversed process in the opposite direction of Equation (1) transfers the superposition of a photon to an atom.

Several conditions must be satisfied for this quantum interface to function. For example, the magnitude of the coupling constant  $g$  must be in the range of the strong coupling

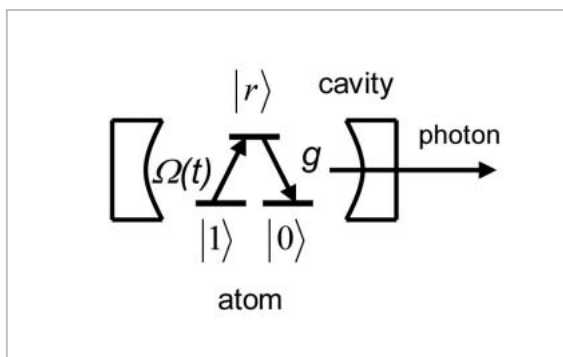


**Fig. 1** Quantum interface based on cavity QED

region (as discussed later); the generated photons must have waveforms with time-reversal symmetry; and the time evolution of the system must satisfy adiabatic conditions [10]. For a photon generated by an atom/cavity system to transmit its superposition to another atom/cavity system, the two systems also need to be indistinguishable in terms of quantum mechanics [10]. Researchers are thus conducting studies using laser-cooled ions and neutral atoms with the difficult aim of constructing a physical system that satisfies all of these conditions.

### 3 Interaction control between the atom and the photon — cavity QED

Here, we describe the coupling between the atom and the cavity in the strong coupling region, which is required to create the atom-photon quantum interface. We also describe a method of generating a single photon featuring the superposition of an atom.

#### 3.1 Strongly coupled atom/cavity system

When an ideal two-level atom is placed in an ideal cavity, the atom and the cavity form a coupled system. This system is known as the Janes-Cummings model. If we denote the coupling constant here as  $g$ , the atom and the cavity coherently exchange an exciton at the frequency  $2g$ , and the energy levels of the first excited states are split by  $2g$ . The quantity  $2g$  is also referred to as the vacuum Rabi frequency. In a practical system, the decay factors ( $\gamma$ ,  $\kappa$ ) are present as shown in Fig. 2, so we thus face a different situation. The dipole induced by the atom decays at the rate  $\gamma$  due to spontaneous emission, and the photon decays at the rate  $\kappa$  due to loss and transmission in the cavity. The time evolution of the coupled atom/cavity system is determined by the magnitude relation between  $g$ , which describes the coherent time evolution, and  $\kappa$  and  $\gamma$ , which describe the decay. If  $g > (\gamma, \kappa)$ , the coherent time evolution is dominant and a system close

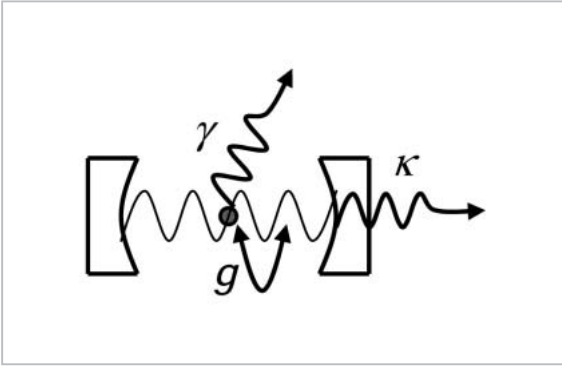


**Fig.2** Atom placed in cavity

to the Janes-Cummings model is realized. This parameter region is referred to as the strong coupling region, and the atom and the cavity are said to form a strongly coupled system. If  $g < (\gamma, \kappa)$ , the decay is dominant. This parameter region is referred to as the weak coupling region. In a weakly coupled atom / cavity system, spontaneous emission from the atom to the cavity is amplified by a factor of  $g^2/\kappa$  (the Purcell effect).

The interaction constant  $g$  between the atom and the cavity is expressed as in the following equation.

$$g(\vec{r}) = \vec{d} \cdot \vec{E}(\vec{r}) = \sqrt{\frac{\mu^2 \omega}{2\hbar \epsilon_0 V_{cav}}} \psi(\vec{r}) \quad (2)$$

Here,  $d$  is the induced dipole of the atom,  $E$  is the light electric field of the single photon normalized in the cavity,  $\mu$  is the dipole moment of the atom,  $\omega$  is the resonance frequency of the cavity,  $\epsilon_0$  is the vacuum permittivity,  $V_{cav}$  is the volume of the cavity, and  $\psi(r)$  is the mode function of the cavity. This equation indicates that the interaction constant  $g$  is a function of the position  $r$  of the atom.

The decay rates  $\kappa$  and  $\gamma$  are given by the following equations.

$$\kappa = \frac{Tc}{2L} \quad (3)$$

$$\gamma = \frac{A}{2} \quad (4)$$

Here,  $T$  is the cavity loss,  $c$  is the speed of light,  $L$  is the length of the cavity, and  $A$  is Einstein's A coefficient.

Equation (2) shows that we need to use a cavity of an extremely small volume to make

$g$  larger than the  $\gamma$  of the atom if we want to realize a strongly coupled system. In such a case, the cavity length  $L$  is also extremely small, which makes  $\kappa$  large, in accordance with Equation (3). To make  $\kappa$  smaller than  $g$ , we need to use a mirror with extremely small loss.

### 3.2 Single photon generation based on cavity QED

As shown in Fig. 1, the atom-photon quantum interface generates a photon that maintains the superposition of the atom by irradiating an appropriate laser pulse to the strongly coupled atom / cavity system. Here, we describe this method for the generation of single photons[11].

Figure 3 shows the energy levels of the atom / cavity system when it generates single photons based on this method. Here, the levels are denoted as  $| \text{atom level, number of photons in the cavity} \rangle$ . An outline of single photon generation is as follows. First,  $|e,0\rangle$  and  $|g,1\rangle$  are strongly coupled by the coupling constant  $g$  with detuning  $\Delta$ . When a laser pulse with the same detuning  $\Delta$  at the Rabi frequency  $\Omega(t)$  is irradiated, the system undergoes unitary (reversible) evolution from  $|u,0\rangle$  to  $|g,1\rangle$ . The photon generated in the cavity is emitted out of the cavity by the transmission of the cavity at the decay rate  $\kappa$ . The whole process of generating a single photon is repeated by initializing the system after the emission of each photon, because repeated emission is

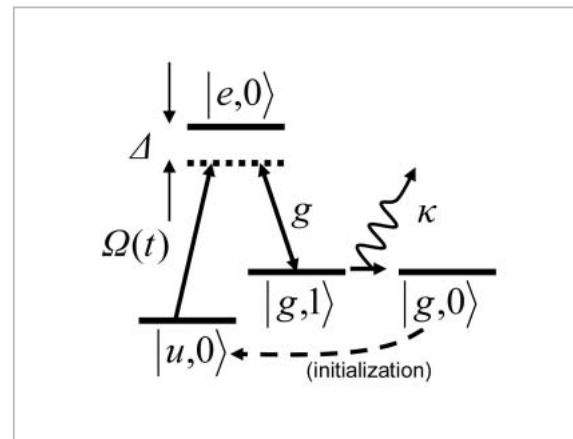


**Fig.3** Single photon generation based on cavity QED

necessary for observation in experiments. Next, we show that this single photon generation is reversible in principle. The eigenstate of the system is expressed as follows, with the perturbation  $g$  and  $\Omega(t)$ .

$$\begin{aligned} |a^0\rangle &= \cos\Theta|u,0\rangle - \sin\Theta|g,1\rangle \\ |a^+\rangle &= \cos\Phi\sin\Theta|u,0\rangle - \sin\Phi|e,0\rangle + \cos\Phi\cos\Theta|g,1\rangle \\ |a^-\rangle &= \sin\Phi\sin\Theta|u,0\rangle + \cos\Phi|e,0\rangle + \sin\Phi\cos\Theta|g,1\rangle \end{aligned} \quad (5)$$

Here,  $\Theta$  and  $\Phi$  are expressed as in the following equations.

$$\begin{aligned} \tan\Theta &= \frac{\Omega(t)}{2g} \\ \tan\Phi &= \frac{\sqrt{4g^2 + \Omega(t)^2}}{\sqrt{4g^2 + \Omega(t)^2 + \Delta^2 - \Delta}} \end{aligned} \quad (6)$$

The state  $|a^0\rangle$  in Equation (5) is a special state that does not contain the contribution of the excited state  $|e,0\rangle$ . The former state is referred to as the dark state and does not cause irreversible spontaneous emission as it does not contain the excited state  $|e,0\rangle$ . Thus, if we adjust  $\Omega(t)$  so that the system does not transit, and let the system adiabatically follow the state  $|a^0\rangle$  such that it undergoes a time evolution of  $|u,0\rangle \leftrightarrow |g,1\rangle$ , a single photon is generated and absorbed reversibly. Equation (6) shows that adjusting  $\Omega(t)$  from  $\Omega(t)=0$  to  $\Omega(t)\gg 2g$  induces unitary time evolution of the state  $|a^0\rangle$  from  $|u,0\rangle$  to  $|g,1\rangle$  and generates a single photon. Using the reverse process, the single photon can be transferred to an atom. This process, based on the dark state, is known as STIRAP (stimulated Raman scattering involving adiabatic passage).

In a real physical system, we have an actual decay rate  $\kappa$  of the cavity and a decay rate  $\gamma$  of the excited atomic state, so the analytical treatment indicated in Equations (5) and (6) cannot be applied as is. The behavior of the system is numerically analyzed using the master equation. The state  $|a^0\rangle$  does not cause spontaneous emission in principle. However, when  $\kappa$  is large, the coherence of  $|a^0\rangle$  is lost and it transits to  $|a^+\rangle$  or  $|a^-\rangle$ , which inevitably causes spontaneous emission. Under these circumstances, it is known that STIRAP only

functions under the strong coupling condition  $g > (\gamma, \kappa)$ . Numerical calculations have predicted that STIRAP generates single photons at a high probability of 90 percent or more in the strong coupling region for both neutral atoms and ions [11][12].

## 4 Present status of laser-cooled-ion-photon quantum network

Two reported experiments have been aimed at implementing an ion-photon interface based on the cavity QED: an experiment by NICT and the Max-Planck Institute of Quantum Optics (MPQ) [6][13], and an experiment by the University of Innsbruck [14]. Here we describe the collaborative experiment by NICT and MPQ.

### 4.1 Steady coupling between single ion and cavity

The interaction constant  $g(r)$  between the single atom and the quantized single mode electromagnetic field is a function of the position  $r$  of the atom in cavity mode, as shown in Equation (2). When the atom couples with the ground state mode, the mode function  $\psi(r)$  in Equation (2) is expressed as in the following equation.

$$\psi(r) = \cos\left(\frac{2\pi z}{\lambda}\right) \exp\left(-\frac{x^2 + y^2}{w_0^2}\right) \quad (7)$$

Here,  $\lambda$  is the wavelength of the mode and  $w_0$  is the spot size of the mode. The axis of the cavity is in the direction of the z-axis. To exercise intentional control over the time evolution of the coupled atom / cavity system,  $g$  must be held constant. To do so, the atom must be confined in the antinodes within a region sufficiently smaller than the wavelength  $\lambda$  of the cavity mode, in accordance with Equations (2) and (7).

We performed an experiment that confined a single  $\text{Ca}^+$  ion in the antinode of a standing wave in a cavity resonating at a wavelength of 397 nm [13]. Figure 4 shows a schematic diagram of the experimental equipment. The cavity consists of two mirrors, each 3 mm in

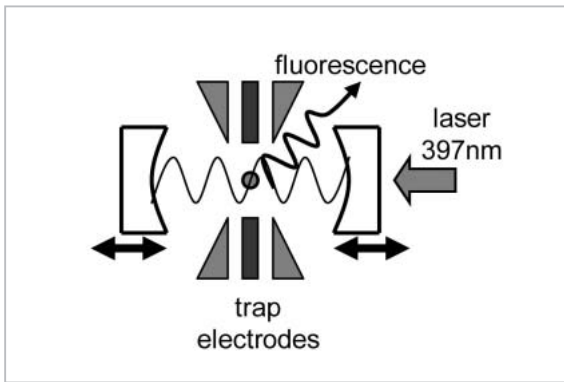


**Fig.4** Experimental equipment for verifying steady coupling between ion and cavity

diameter and 10 mm in length. The tips of the mirrors are tapered to 1 mm in diameter. The curvature radius of each mirror surface is 10 mm. The mirrors are placed apart at a distance of 6 mm. The measured finesse is approximately 3,000. The linear ion trap consists of four rf electrodes and a DC electrode that controls the ion motion on the trap axis. The ion trap is operated at a frequency of 13 MHz and an amplitude of 400 V. The position of the cavity is controlled using a three-axis piezostage such that the center of the cavity approximately aligns with the center of the ion trap. The single  $\text{Ca}^+$  ion generated out of the cavity is introduced into the cavity and placed near the center by the DC electrodes. The  $\text{Ca}^+$  ion is laser-cooled (i.e., Doppler cooled) using laser light at a wavelength of 397 nm, and is localized. The cavity is coupled with weak laser light resonating with the  $\text{Ca}^+$  ion, and the ground state mode expressed in Equation (7) is excited. The  $\text{Ca}^+$  ion emits fluorescence proportional to the intensity of the light electric field at the position of the ion. If we measure the fluorescence intensity distribution by scanning the position of the  $\text{Ca}^+$  ion, we should be able to estimate the degree of localization from the visibility of the distribution.

Figure 5 shows the fluorescence pattern measured by scanning the relative position of the ion, which is itself accomplished by scanning the position of the cavity. A standing wave pattern at the wavelength of 397 nm is

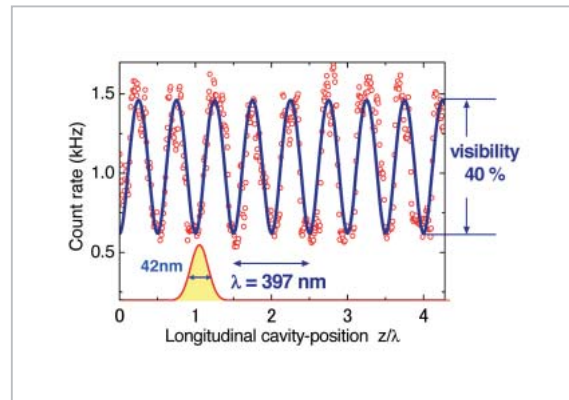


**Fig.5** Fluorescence pattern emitted by  $\text{Ca}^+$  ion in cavity

well distinguished, which indicates that the  $\text{Ca}^+$  ion is localized in a region sufficiently smaller than this wavelength. From the analysis of visibility, we found that the full width at half maximum of the wave packet of the  $\text{Ca}^+$  oscillation is 42 nm. The temperature here is determined to be 0.6 mK, which is slightly higher than the Doppler limit temperature (0.5 mK). With the range of the localization of the ion obtained, the fluctuation of the coupling  $g$  between the ion and the cavity at the wavelength of 866 nm, which is used in the experiment discussed later, is 2 percent or less. We were able to trap the  $\text{Ca}^+$  ion for more than 90 minutes in this state. This experiment confirms that combining the simplest Doppler cooling and strong constraining force by the ion trap can localize an atom in a region sufficiently smaller than the wavelength within a microcavity and can maintain the ion-cavity coupling constant  $g$  unchanged.

## 4.2 Single photon generation by single-ion-cavity system

To implement the atom-photon quantum interface of Reference [10], we need to construct a system in which the atom and the microcavity are strongly coupled and which can generate a single photon according to the excitation pulse. As a first step toward implementation, we performed an experiment in which a single photon was generated at a wavelength of 866 nm [6] using a  $\text{Ca}^+$  ion coupled with the microcavity, based on the

method described in Reference[11]. Figure 6 (a) shows a schematic diagram of the experimental equipment. Figure 6 (b) shows the energy levels of the  $\text{Ca}^+$  ion. The single  $\text{Ca}^+$  ion is coupled within a microcavity resonating at a wavelength of 866 nm and is excited with a pulse of wavelength 397 nm to generate the single photon.

We performed this experiment with nearly the same equipment as the experiment discussed earlier, with the exception of the cavity. The cavity in this experiment has an asymmetric structure consisting of two mirrors with transmittance of 600 ppm and 5 ppm, respectively, at a wavelength of 866 nm. In this manner, the photon generated is emitted in one direction. The distance between the mirrors is 8 mm. The parameters that describe the system here are  $(g, \kappa, \gamma) = 2\pi(0.92, 1.2, 0.85)\text{MHz}$ ; these conditions do not place us in the strong coupling region. After the  $\text{Ca}^+$  ion is localized in the antinode of the cavity mode, it is irradiated with laser light at a wavelength of 397 nm shaped by an acoustooptic modulator, and a single photon is generated. After single photon generation, an initializing laser pulse is inserted, and single photon generation is repeated at a frequency of 100 kHz. The single photons

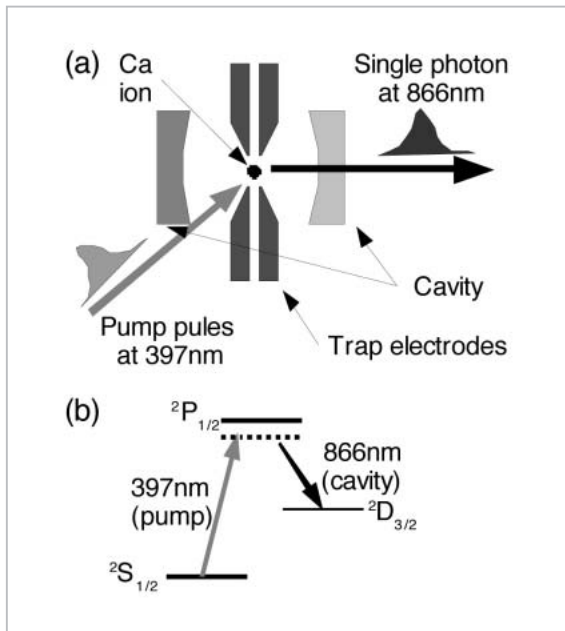
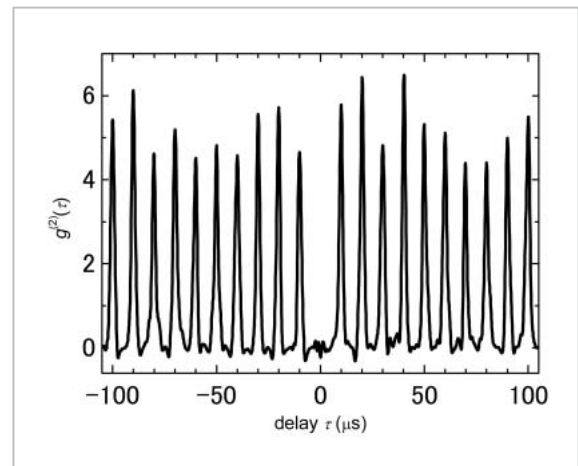


**Fig.6** (a) Experimental equipment for generating single photon and (b) energy levels of  $\text{Ca}^+$  ion

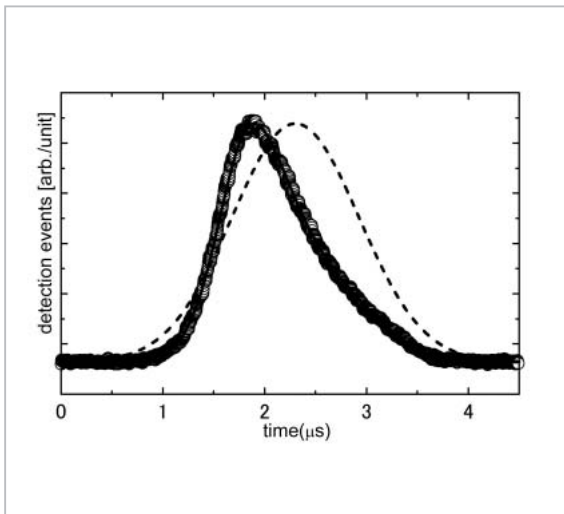
are detected with an avalanche photodiode (APD). All detection times are recorded and the results are analyzed.

Figure 7 shows the second-order coherence function  $g^{(2)}(\tau)$  measured by a Hanbury Brown-Twiss interferometer consisting of two APDs and a 50:50 beam splitter. The dark count rate is too large to neglect compared with the number of single photons, so the contribution of dark counts is subtracted in the figure using a correlation formula for the dark count rate and the number of single photons[6]. The value at time difference  $\tau=0$  is  $g^{(2)}=0$ , which proves that the observed photon is a single photon. A peak is observed in the correlation frequency every 10 microseconds because the single photon is generated repeatedly at a frequency of 100 kHz. Single photons generated by the same ion are observed for 3,000 seconds, amounting to  $411,200 \pm 335$  counts. The number of events in which two photons may be detected simultaneously is  $2 \pm 13$  times.

We reconstruct the waveform of the generated single photon by plotting the relationship between the frequency at which a single photon is detected and the detection time. Figure 8 shows the waveform of the single photon generated by a Gaussian pump pulse. The waveforms observed are indicated by circles, which agrees well with the simulated waveform, indicated by the black solid curve, derived from the master equation. This shows that the



**Fig.7** Second-order coherence function of observed single photons



**Fig.8** Time waveform of single photon

experimental system corresponds to a physical system that agrees well with the model described by the master equation [12].

It is characteristic of a coupled ion-cavity system that it can maintain a steady coupled state for a long time. Thus, by controlling the waveform  $\Omega(t)$  of the pump pulse, we can perform active control of the waveform of the generated single photon. To demonstrate this characteristic, we observe the waveforms of the single photons generated by pump pulses of various waveforms. Figure 9 shows examples. In (a), a pump pulse with two peaks is used and a single photon is generated with two peaks in the time waveform. In (b), a weak Gaussian pump pulse is used and a single photon is generated with time-reversal symmetry in the waveform. The gray solid curves indicate the waveforms of the pump pulses, the circles indicate the measured values, and the black solid curves are waveforms predicted by the master equation. The predicted and measured time waveforms agree well in both cases.

Based on the quantum efficiency of APD, the transmittance of the light path guiding the single photon to the APD, and the frequency at which a single photon is observed, we estimate the probability of generation of a single photon in relation to the single pump pulse. The result is approximately 8 percent. This value is considerably smaller than the proba-

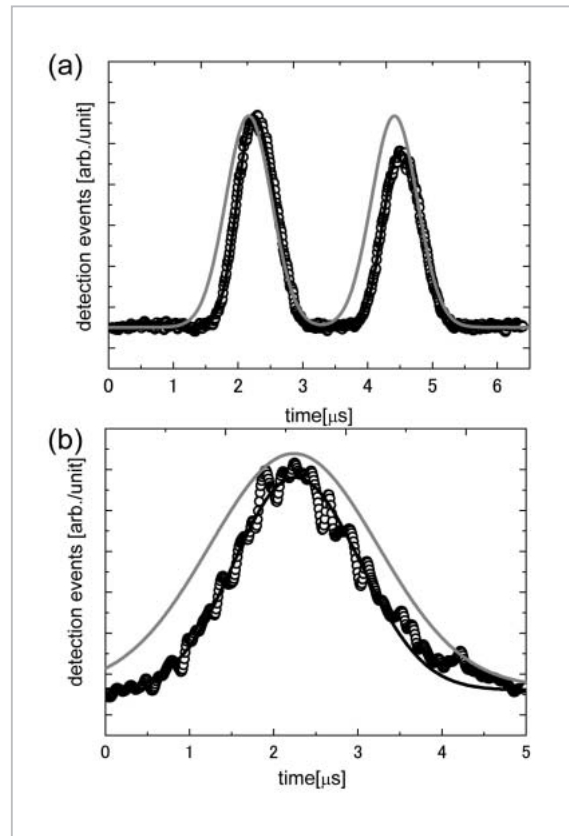


**Fig.9** Time waveform of single photon generated by (a) pump pulse with two peaks and (b) pump pulse with weak Gaussian waveform

bility of 90 percent predicted for single photon generation by STIRAP. This is due to the fact that the ion-cavity system does not form a strongly coupled system in this experiment. The coupling constant  $g$  depends on the cavity length  $L$  as follows.

$$g \propto L^{-3/4} \quad (8)$$

In principle, we can make  $g$  larger by decreasing the cavity length. However, in reality, the mirror surface, which is a dielectric body, exerts an external disturbance on ion trap potential, such that  $L = 8$  mm is the lower limit of cavity length required to maintain the ion in a stable state with the ion trap used in the experiment.

### 4.3 Conditions for implementing ion-photon quantum interface

Although we have successfully generated a single photon with a controlled time waveform using a system in which a single  $\text{Ca}^+$  ion

stably couples with the microcavity, the conditions under which an atom-photon quantum state interface is generated as indicated in Reference[10] are not satisfied. The parameters that characterize the system consisting of a single ion and a microcavity are  $(g, \kappa, \gamma) = 2\pi (0.92, 1.2, 0.85)$  MHz, in which  $g$ , which determines the coherent evolution of the system, is comparable to the decay constants  $\kappa$  and  $\gamma$ . This is also why the probability of single photon generation is as low as 8 percent. The strong coupling condition for the quantum interface to function is  $g > (\kappa, \gamma)$ .

Now, can we not carry the superposition of the ion using the single photon generated in the experiment, though this may be at a low probability? To solve this problem, we perform two types of analysis: analysis based on the master equation and analysis based on the quantum-jump approach[15]. While the former analysis calculates the time evolution of the quantum system, including events in which the system experiences decay, the latter analysis excludes events in which the system has experienced decay and calculates only the unitary time evolution of the system. Figure 10 shows the results of single photon waveform simulation performed under conditions close to those of the experiment. The gray solid curve indicates a solution based on the master equation, and the black solid curve indicates a solution based on the quantum-

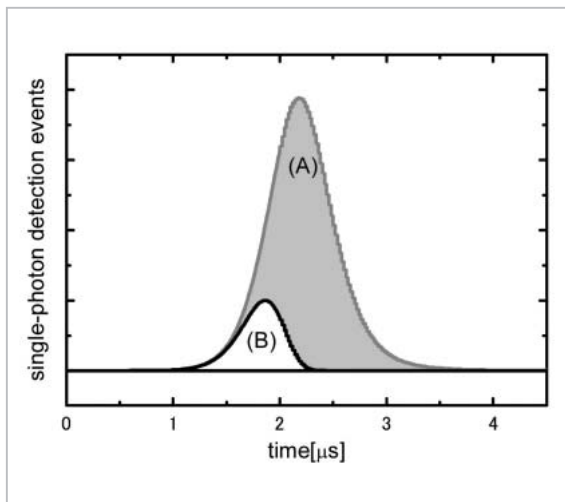


**Fig. 10** Single photon waveform simulation

jump approach. The photons observed in the experiment follow the master equation and correspond to the sum of the area filled with gray (A) and the area filled with white (B) in Fig. 10. A more detailed calculation has clarified that among these two areas, the photons in (A) in Fig. 10 are generated after one or more spontaneous emissions between  ${}^2P_{1/2}$ - ${}^2S_{1/2}$ , as indicated in Fig. 11 (a). The spontaneous emissions erase the superposition of the ions, so the system does not function as an ion-photon quantum interface. The photons in (B) in Fig. 10, which correspond to 17 percent of the observed photons, are generated through unitary time evolution, as indicated in Fig. 11 (b), and can transfer the quantum states of the ion. Together with a single photon generation probability of 8 percent, the present experimental equipment can transfer the quantum state from the ion to the photon at a probability of 1.4 percent per single pump pulse. However, the photon detection efficiency of the experimental system is 4.5 percent and can detect only 63 events per second, even if the experiment is performed repeatedly at a frequency of 100kHz. As the dark count of the APD is 50 counts per second, which is approximately the same order of frequency, we need to generate unitary photons at a higher probability if we are to confirm experimentally the transfer of quantum states.

To generate unitary photons using a  $\text{Ca}^+$

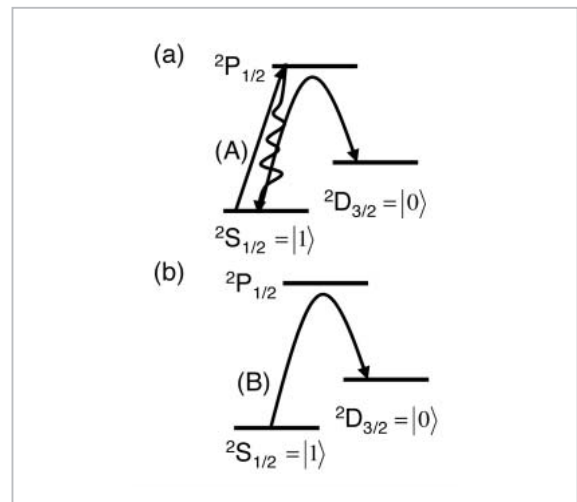


**Fig. 11** Processes of single photon generation

ion, we must avoid the process accompanied by spontaneous emissions indicated in Fig. 10 (a). The condition is  $g > \Gamma$ , where  $\Gamma$  is the dipole decay rate of  ${}^2P_{1/2} - {}^2S_{1/2}$ . As the decay rate of  ${}^2P_{1/2} - {}^2D_{3/2}$ ,  $\gamma$ , is  $2\pi \cdot 0.85$  MHz, and  $\Gamma$  is  $2\pi \cdot 11$  MHz, together with the strong coupling condition,  $g > (\kappa, \gamma)$ , it is sufficient that  $g > (\kappa, \Gamma)$  be satisfied. The method for satisfying this condition is to implement the following conditions at the same time: to increase  $g$  by decreasing the cavity length  $L$ , as indicated in Equation (8), and to suppress  $\kappa$  using mirrors with low loss  $T$ , as indicated in Equation (3). As a guideline, let us consider a cavity with a length of 0.1 mm and loss of 10 ppm. The parameters are then  $(g, \kappa, \Gamma) = 2\pi (15, 2.4, 11)$  MHz, which satisfies the required condition. Here, a simulation based on the quantum-jump approach predicts that the ion-photon quantum interface functions at a probability of approximately 90 percent. In order to avoid disturbance of ion motion by mirrors separated by a small distance, the ion trap used here must feature a structure in which electrodes are placed in the cavity in such a manner as to shield the ions from the mirrors to the full extent possible.

## 5 Future perspectives

In quantum computation based on laser-cooled ions, implementation of large-scale computation, including error correction, has recently become a popular research topic. Thus, it has become a significant challenge to develop a micro-ion-trap that integrates quantum-gate and memory regions in a single trap<sup>[16]</sup>. A recently reported operating micro-ion-trap is based on semiconductor process technology and features an electrode interval of  $60\mu\text{m}$ <sup>[16]</sup>. It is hoped that combining trap equipment of this type and a microcavity with a distance between mirrors of approximately 0.1 mm can provide a strongly coupled system offering high-probability operation of the ion-photon quantum interface.

Instead of using an ion-photon quantum interface, we may consider constructing a quantum network by establishing quantum entanglement between remote ions and using quantum teleportation. The problem with this method lies in the formation of quantum entanglement between remote ions. If a photon entangled with an ion is generated in single space mode based on the weakly coupled cavity QED<sup>[17]</sup>, and if Bell measurement is performed between this photon and another photon generated by the same method at a remote location, quantum entanglement is believed to form probabilistically between the ions by entanglement swapping<sup>[18]</sup>. The requirement of the photons used in this method is that they be indistinguishable, which is not as strict as the requirements governing the ion-photon quantum interface. Experimentally, quantum entanglement has been observed between the basic resources of the single ion and the single photon<sup>[19]</sup>. As such, quantum teleportation based on probabilistically generated quantum entanglement between ions is also a promising candidate as a practical method of constructing a quantum network.

NICT is continuing research for the implementation of a quantum network, based on single photon generation technology established by NICT in collaboration with MPQ, involving the combination of a single ion and an optical cavity. NICT has adopted two approaches in this endeavor: one based on the ion-photon quantum interface and another based on quantum teleportation. If a physical system consisting of a micro-ion-trap and a microcavity with extremely low loss can generate either unitary photons or photons in quantum entanglement with ions, a prototype quantum network based on ions and photons should operate functionally. With this prototype, we expect that we will be able to demonstrate operation of a quantum information communication protocol that can be realized only by faithful exchange of quantum states.

---

## References

- 1 M.Sasaki, "3-1 Overview of Quantum Info-Communications and Research Activities in NICT", This Special Issue of NICT Journal.
- 2 H. Yonezawa, T. Aoki, and A. Furusawa, Nature 431, 430, 2004.
- 3 C. Monroe, Nature 416, 238, 2002.
- 4 W. Yao, R. B. Liu, and L. J. Sham, Phys. Rev. Lett. 95, 030504, 2005.
- 5 H. Häffner et al, Nature 438, 643, 2005 ; Leibfried, D. et al. Nature 438, 639, 2005.
- 6 M. Keller, B. Lange, K. Hayasaka, W. Lange, and H. Walther, Nature 431, 1075, 2004.
- 7 P. T. H. Fisk, M. J. Sellars, M. A. Lawn, C. Coles, A. G. Mann, and D. G. Blair et al., IEEE Trans. Instrum. Meas. 44, 113, 1995.
- 8 C. Langer, et al, Phys. Rev. Lett. 95, 060502, 2005.
- 9 J. I. Cirac, P. Zoller, Phys. Rev. Lett. 74, 4091, 1995.
- 10 J. I. Cirac, P. Zoller, H. J. Kimble, and H. Mabuchi, Phys. Rev. Lett. 78, 3221, 1997.
- 11 A. Kuhn, M. Hennrich, T. Bondo, and G. Rempe, Appl. Phys. B 69, 373, 1999.
- 12 M. Keller, B. Lange, K. Hayasaka, W. Lange, and H. Walther, New Jour. Phys. 6, 95, 2004.
- 13 G. R. Guthöhrlein, M. Keller, K. Hayasaka, W. Lange, and H. Walther, Nature 414, 49, 2001.
- 14 A. B. Mundt, A. Kreuter, C. Becher, D. Leibfried, J. Eschner, F. Schmidt-Kaler, and R. Blatt, Phys. Rev. Lett. 89, 103001, 2002.
- 15 M. B. Plenio and P. L. Knight, Rev. Mod. Phys. 70,101, 1998.
- 16 D. Stick, W. K. Hensinger, S. Olmschenk, M. J. Madsen, K. Schwab, and C. Monroe, Nature Physics 2, 36-39, 2006.
- 17 B. Sun, M. S. Chapman, and L. You, Phys. Rev. A 69, 042316, 2004.
- 18 C. Simon, T. Irvine, Phys. Rev. Lett. 91, 11405, 2003.
- 19 B.B. Blinov, D.L. Moehring, L.-M. Duan, and C. Monroe, Nature 428, 153, 2004.



**HAYASAKA Kazuhiro**

*Senior Researcher, Advanced Communications Technology Group, New Generation Network Research Center (former : Senior Researcher, Quantum Information Technology Group, Basic and Advanced Research Department)  
Quantum Optics, Quantum Information*

**KELLER Matthias, Ph.D.**

*Academic Staff, Max-Planck-Institute of Quantum Optics  
Quantum Optics*

**LANGE Birgit, Ph.D.**

*Academic Staff, Max-Planck-Institute of Quantum Optics  
Quantum Optics*

**LANGE Wolfgang, Ph.D.**

*Academic Staff, Max-Planck-Institute of Quantum Optics  
Quantum Optics*

**WALTHER Herbert, Ph.D.**

*Academic staff, Max-Planck-Institute of Quantum Optics  
Quantum optics*